International Research Journal of Advanced Engineering and Science
ISSN (Online): 2455-9024

Inverse Dynamics Analysis of the Robot Arm Using the Topology Optimization

Duong Xuan Bien, Pham Dac Phong, Pham Hoang Nam, Le Thanh Hung
Advanced Technology Center, Le Quy Don Technical University, Hanoi, Vietnam

***Abstract*—** *This paper presents the results of the inverse dynamics analysis of the two degrees of freedom (2DOF) robot arm with the topology optimized (TO) links. Static and dynamic models of the robot arm are analyzed to determine the force and moment values acting on the joints under the impact of loads on the end-effector link. The robot position with the largest loads is determined. Accordingly, the structural optimization technique is used to optimize the links with specific criteria of mass reduction, stress and displacement. The inverse dynamics (IK) problem is solved for two cases before and after the optimization based on building a mathematical model and dynamic equations of the robot. The joints driving torques values are compared in both cases. The survey results showed that, with the weight reduction of the joints reaching over 40%, the maximum value of joints driving torques reduced by more than 43% in a positive direction with the tendency to decrease the load bearing level of the joints and increase the life of joints. The research content has important implications in optimizing the design with the reduction of material costs and improving the working efficiency of the structures in general and the robotic system in particular.*

***Keywords*—** *Driving energy, robot arm, topology optimization, dynamics modelling.*

I. INTRODUCTION

In the current and near future, the number of robots will be used widely with continuous operation frequency and long working cycles in smart factories. Therefore, they are subject to high energy consumption in production. Finding solutions to reduce energy consumption is an urgent matter in order to minimize costs and enhance production efficiency. The problem of reducing costs and improving machining productivity of robots is solved in many directions such as optimization of machining trajectory [1], feed rate [2], technology parameters [3] and reduction of machining time leads to reduced energy consumption during total process [4].

In the overall energy consumption problem, the driving torques at joints accounts for a fairly high percentage because they are directly related to the actuators and their corresponding efficiency. The links weight in particular and the robot motion trajectory in general have a great influence on the consumption of driving torques [5]. Structural designing to reduce the links weight has also been considered recently such as the flexible robot study [6], the optimization techniques application in the structural design [7]. First of all, the trend of reduced mass is always considering for almost objects moving because the lighter, the more energy efficient. With the robot structure, the lighter the components of the robot, the better it is to save construction materials, reduce inertia in motion, reduce the cost of driving energy, and reduce the load-bearing level of the actuators, convenient in moving between working place. Mass reduction becomes especially important for flying devices. Basically, structurally optimized parts will often require less resources to create them such as materials, energy to manufacture, manufacturing processes, sometimes space occupied in the working place. Therefore, optimizing structures using TO technique is still essential.

In particular, the TO method [8-21] is preferred to reduce the structural weight of the robot but still ensure the load capacity, control the stress and deformation state of the system. The procedure for performing simple TO is described in [8]. The Solid Isotropic Material with Penalization (SIMP) method for isotropic materials is clearly presented in [9], [10]. The Bi-Evolutionary Structural Optimization (BESO) method is mentioned in [11]. The LEVELSET method is shown in [12]. TO algorithms are applied in many different fields and objects such as in truss structures [13], Vehicle [14], Humanoid robot [15], Quadcopter [16] and industrial robot (IR) arms [17-20]. SIMP method was used in [17] to optimize the Upper Arm (UA) link on 6DOF industrial robot with a weight reduction of 44.4% but it is not clearly yet. The multi-objective TO problem including stiffness, vibration frequency and IR mass was performed in [18] with the UA link being optimally selected. Similarly, the multi-objective TO problem is also considered for the IR in [19] with the SIMP method. A mainly link on the IR arm is optimally analyzed in [20] based on Generative Design (GD) module and TO method for additive manufacturing (AM). The mechanical and microstructural properties of the part using AM were analyzed to evaluate the optimal design quality with a 50% reduction in the weight of the part.

The main contribution of this paper is the investigation results of the driving torque value of the joints on two-link planar robot using SIMP technique for 2nd link under the impact of loads on the end-effector point (EEP). The material of links is defined to Aluminum 6061. The statics and dynamics model of the robot are considered in order to find the force and moment values for the optimal expected link. The criteria of mass, stress and displacement are proposed to correspond to the boundary conditions of the optimization problem. The driving torque values of joints in the cases Pre-TO and After-TO are compared through the IK and ID problems. Quantitative results of the driving torque will be the basis for developing the application of TO technique to most other components of the robot or to other similar systems.

II. MATERIALS AND METHODS

A. Static and dynamic analysis for 2DOF robot pre-TO

Duong Xuan Bien, Pham Dac Phong, Pham Hoang Nam, and Le Thanh Hung, "Inverse Dynamics Analysis of the Robot Arm Using the Topology Optimization," *International Research Journal of Advanced Engineering and Science*, Volume 8, Issue 1, pp. 267-272, 2023.

International Research Journal of Advanced Engineering and Science
ISSN (Online): 2455-9024

Consider a two-link planar robot model as shown in Fig. 1. The local coordinate systems $(OXYZ)_1$ and $(OXYZ)_2$ are attached to the starting points of links 1 and 2, respectively. The lengths of the links are L_1 and L_2. The distances from the local origin to the centroid along the links lengths are L_{G1} and L_{G2}. The load applied at the end-effector point (E point) is $F = 10(N)$. The weights of the links are G_1 and G_2, respectively. The angle between the links and the horizontal is α and β, respectively.

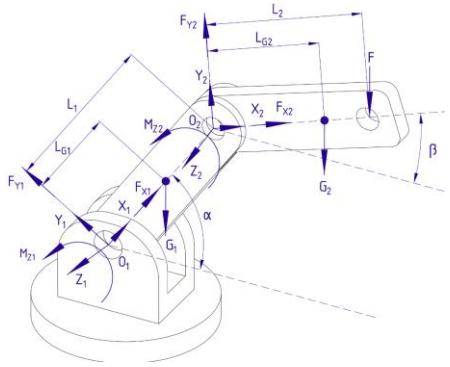

Fig. 1. Static analysis model

The static equations are defined as follows

$$\sum F_{xi} = 0; \sum F_{yi} = 0; \sum F_{zi} = 0;$$
$$\sum M_{xi} = 0; \sum M_{yi} = 0; \sum M_{zi} = 0; \quad (1)$$
$$(i = 1,2)$$

At joint 1

$$\begin{cases} F_{X1} = (G_1 + G_2 + F)\sin\alpha \\ F_{Y1} = (G_1 + G_2 + F)\cos\alpha \\ M_{Z1} = \left(L_{G1}G_1 + L_1G_2 + L_1F\right)\cos\alpha \\ \qquad + \left(L_{G2}G_2 + L_2F\right)\cos\beta \end{cases} \quad (2)$$

At joint 2

$$\begin{cases} F_{X2} = (G_2 + F)\sin\beta \\ F_{Y1} = (G_2 + F)\cos\beta \\ M_{Z1} = \left(L_{G2}G_2 + L_2F\right)\cos\beta \end{cases} \quad (3)$$

In fact, force and torque greatly affect the working condition of the robot. In which, moment has the most influence on stress and displacement of joints and joints. It is easy to see, M_{Z1} and M_{Z2} are greatest when $\alpha = \beta = 0^0$ or $\alpha = \beta = 180^0$. The geometric parameters of the model include

$L_1 = 0.25(m);$

$L_{C1} = 0.115(m); L_2 = 0.19(m); L_{C2} = 0.097(m);$
$G_1 = 10(N); G_2 = 4.48(N); \alpha = 0; \beta = 0;$ $F = 10(N)$.

Accordingly, the force and moment values at the respective position are determined as follows

$F_{X1} = 0; F_{Y1} = 24.48(N); M_{Z1} = 8.486(Nm);$
$F_{X2} = 0; F_{Y2} = 14.48(N); M_{Z2} = 2.34(Nm);$

Consider the dynamic analysis problem with the start position (P1) corresponding to $\alpha = \beta = 0^0$ and the material of links is aluminum 6061. Joint 1 and joint 2 are driven with velocities $v_1 = \frac{\pi}{12}(rad/s)$ and $v_2 = \frac{\pi}{18}(rad/s)$ respectively. Fig. 2 (a, b, c) describes the corresponding position of the robot on the moving trajectory (start position, middle position and end position).

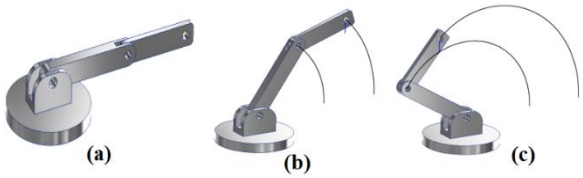

Fig. 2. Motion positions of 2DOF robot in pre-TO

Based on the above motion trajectory, the force and moment values acting on joints 1 and 2 are specifically determined as shown in Fig. 3 and Fig. 4, respectively.

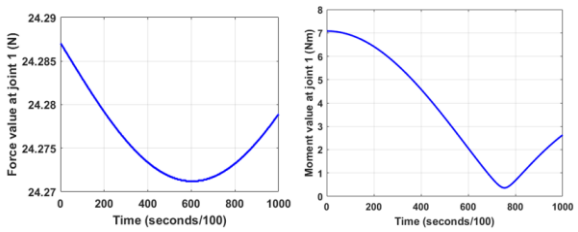

Fig. 3. Force and moment values at joint 1

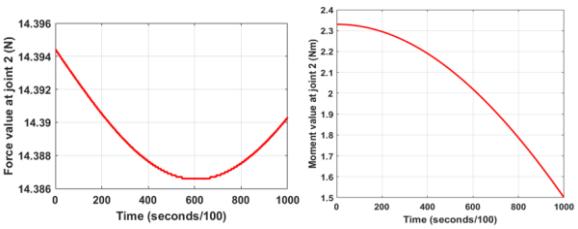

Fig. 4. Force and moment values at joint 2

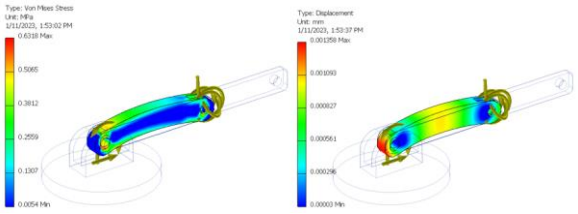

Fig. 5. Stress and displacement values of link 1 at start point

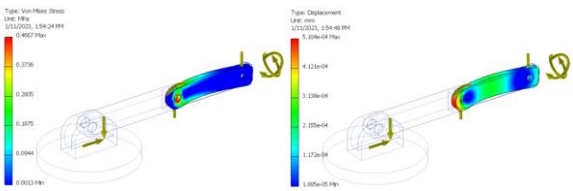

Fig. 6. Stress and displacement values of link 2 at start point

Duong Xuan Bien, Pham Dac Phong, Pham Hoang Nam, and Le Thanh Hung, "Inverse Dynamics Analysis of the Robot Arm Using the Topology Optimization," *International Research Journal of Advanced Engineering and Science*, Volume 8, Issue 1, pp. 267-272, 2023.

Accordingly, the maximum force and moment values acting on joint 1 are 24.29 (N) and 7.08 (Nm), respectively. These values at joint 2 are obtained at 14.39 (N) and 2.34 (Nm). It is easy to see that the maximum force and torque values acting on the joints at 1 position in the case of static analysis differ very little compared to the case of dynamic analysis. Fig. 5 and Fig. 6 describe the stress and displacement values of link 1 and link 2 corresponding to the initial position in the motion trajectory. This position is most affected by force and moment. This numerical simulation result is determined based on the finite element analysis (FEA) module of the INVENTOR software.

B. Optimizing the structure of the two-link planar robot

In this study, the structure of link 2 was optimized by SIMP technique [7], [8], [19] with some basic parameters including meshing (200), reduce originally (50%), external force (10N), density (2700 kg/m^3), poisons modulus (0.33) and young's modulus (70 GPa). The results of link 2 topology optimization are shown in Fig. 7.

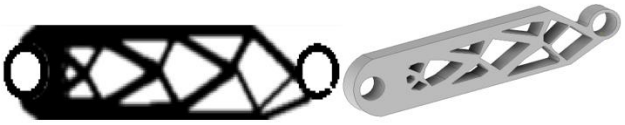

Fig. 7. Optimal results of link 2 using SIMP

Perform the dynamic analysis problem with the motion trajectory of the robot as described in section 2.1. The simulation and analysis of force/moment acting on results the joints are described from Fig. 8 to Fig. 12. The comparison results before and after optimization are presented in detail below.

Fig. 8. Motion positions of 2DOF robot in after-TO

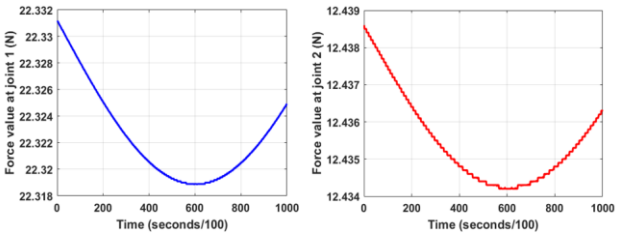

Fig. 9. Force values at joint 1 and joint 2

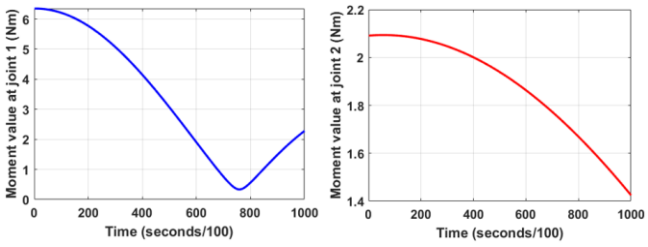

Fig. 10. Moment values at joint 1 and joint 2

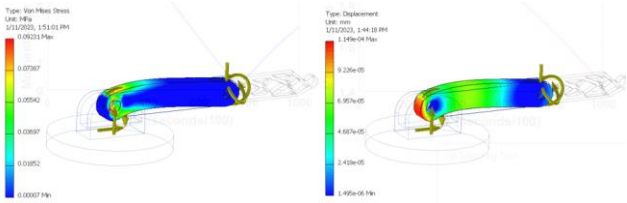

Fig. 11. Simulation results of stress and displacement at joint 1

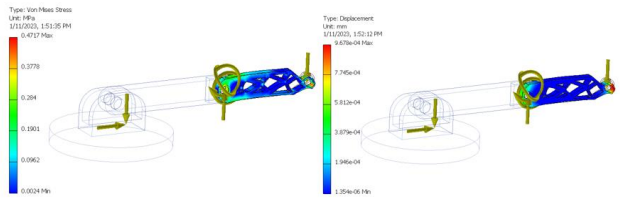

Fig. 12. Simulation results of stress and displacement at joint 2

The force and moment values in the problems of static and dynamic analysis in the two cases are shown in detail in Tab. 1.

TABLE I. STATIC AND DYNAMIC ANALYSIS RESULTS BEFORE AND AFTER OPTIMIZATION

Static analysis results at $\alpha = \beta = 0^0$				
Max. Value	**Joint 1**		**Joint 2**	
	Force (N)	***Moment (Nm)***	***Force (N)***	***Moment (Nm)***
Pre-TO	24.48	8.486	14.48	2.336
After-TO	22.49	8.235	12.49	2.085
Deviation	Reduced 8.13%	Reduced 2.96%	Reduced 13.74%	Reduced 10.74%
Dynamic analysis results at $\alpha = \beta = 0^0$				
Max. Value	**Joint 1**		**Joint 2**	
	Force (N)	***Moment (Nm)***	***Force (N)***	***Moment (Nm)***
Pre-TO	24.287	7.08	14.394	2.33
After-TO	22.33	6.35	12.438	2.09
Deviation	Reduced 8.06%	Reduced 10.31%	Reduced 13.59%	Reduced 10.3%

It is easy to see that the static and dynamic analysis results at the position of the largest load have no significant difference. On the other hand, the after-optimal moment and force values tend to decrease. The reduction level at joint 1 was less than 11% and at joint 2 was less than 14%. Based on these maximum force and moment values, the maximum stress and displacement (Dis.) values are determined through the FEA module. The results of the analysis are described in Tab. 2.

TABLE II. RESULTS OF ANALYSIS OF MAXIMUM STRESS AND DISPLACEMENT

Max. Value	**Link 1**		**Link 2**	
	Stress (MPa)	***Dis. (mm)***	***Stress (MPa)***	***Dis. (mm)***
Pre-TO	0.632	13.58×10^{-4}	0.467	5.1×10^{-4}
After-TO	0.092	1.15×10^{-4}	0.471	9.67×10^{-4}
Deviation	Reduced 0.54	Reduced 12.43×10^{-4}	Reduced 0.004	Reduced 4.57×10^{-4}

The maximum stress and displacement values on link 1 are significantly reduced. In contrast, these values increase above

Duong Xuan Bien, Pham Dac Phong, Pham Hoang Nam, and Le Thanh Hung, "Inverse Dynamics Analysis of the Robot Arm Using the Topology Optimization," *International Research Journal of Advanced Engineering and Science*, Volume 8, Issue 1, pp. 267-272, 2023.

link 2. However, the increase is very small ($4\times10^{-3}MPa$ and $4.57\times10^{-4}mm$). These results completely meet the topology optimization criteria set out initially.

The maximum stress and displacement values on link 1 are significantly reduced. In contrast, these values increase above link 2. However, the increase is very small ($4\times10^{-3}MPa$ and $4.57\times10^{-4}mm$). These results completely meet the topology optimization criteria set out initially.

C. Driving torque determination of two-link planar robot

Mathematical model and DH parameters of a two-link planar robot are depicted in Fig. 13. In which, $(OXY)_0$ is a fixed coordinate system. $(OXY)_1$ and $(OXY)_2$ are coordinate systems associated with links 1 and 2, respectively. The end-effector point is E with the position vector in coordinate system $(OXY)_0$ being $\mathbf{x}_E = \begin{bmatrix} x_E & y_E \end{bmatrix}^T$. The load acting on the robot is P_L and is placed at point E. Points C_1 and C_2 are the centroid positions of the links. The mass and length of the links are m_1, m_2 and L_1, L_2, respectively. The driving torques of the joints are τ_1 and τ_2. The rotation angles of the joints are q_1 and q_2, respectively. The joint variable vector is $\mathbf{q} = \begin{bmatrix} q_1 & q_2 \end{bmatrix}^T$.

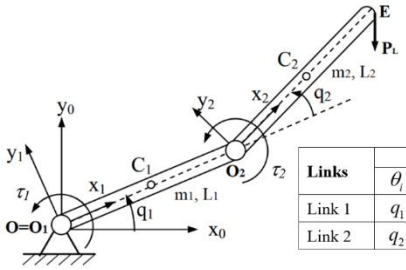

Links	DH parameters			
	θ_i	d_i	a_i	α_i
Link 1	q_1	0	L_1	0
Link 2	q_2	0	L_2	0

Fig. 13. Mathematical model and DH parameters of a two-link planar robot

The kinematics and dynamics equations of 2DOF robot is easily determined according to [21]

$$\begin{aligned} x_E &= L_1\cos q_1 + L_2\cos(q_1+q_2); \\ y_E &= L_1\sin q_1 + L_2\sin(q_1+q_2) \end{aligned} \tag{4}$$

And

$$\mathbf{M}(\mathbf{q})\ddot{\mathbf{q}} + \mathbf{C}(\mathbf{q},\dot{\mathbf{q}})\dot{\mathbf{q}} + \mathbf{g}(\mathbf{q}) = \boldsymbol{\tau} + \mathbf{Q}^* \tag{5}$$

In which, $\mathbf{M}$ is the mass matrix, $\mathbf{C}(\mathbf{q},\dot{\mathbf{q}})$ is the Coriolis matrix, and $\mathbf{g}(\mathbf{q})$ is the gravitational potential energy matrix. The components of the dynamic equation are determined as follows

$$\begin{aligned} &\mathbf{M} = \begin{bmatrix} m_{11} & m_{12} \\ m_{21} & m_{22} \end{bmatrix}; \mathbf{g}(\mathbf{q}) = \left(\frac{\partial \Pi}{\partial \mathbf{q}}\right)^T; \boldsymbol{\tau} = \begin{bmatrix} \tau_1 & \tau_2 \end{bmatrix}^T \\ &\mathbf{C}(\mathbf{q},\dot{\mathbf{q}}) = \frac{\partial \mathbf{M}(\mathbf{q})}{\partial \mathbf{q}}(\mathbf{I}_n \otimes \dot{\mathbf{q}}) - \frac{1}{2}\left(\frac{\partial \mathbf{M}(\mathbf{q})}{\partial \mathbf{q}}(\dot{\mathbf{q}} \otimes \mathbf{I}_n)\right)^T; \end{aligned} \tag{6}$$

In which, the elements of matrix A are determined as follows

$$\begin{aligned} m_{11} &= m_1 L_{G1}^2 + m_2(L_1^2 + L_{G2}^2 + 2L_1 L_{G2}\cos q_2) \\ &\quad + I_{2Z} + I_{1Z} \\ m_{12} &= m_{21} = m_2(L_{G2}^2 + 2L_1 L_{G2}\cos q_2) + I_{2Z}; \\ m_{22} &= m_2 L_{G2}^2 + I_{2Z} \end{aligned} \tag{7}$$

The expression for the total potential energy of the system is presented as follows

$$\begin{aligned} \Pi &= m_1 g L_{G1}\sin q_1 \\ &\quad + m_2 g(L_1\sin q_1 + L_{G2}\sin(q_1+q_2)) \end{aligned} \tag{8}$$

The load attached at the E point with mass m_{Load} is considered an external force $P_L = m_{Load}g(N)$. Therefore, the virtual work δA of the generalized force P_L is determined as follows

$$\delta A = \tau_1\delta q_1 + \tau_2\delta q_2 - P_L\delta y_E \tag{9}$$

And

$$\begin{aligned} \delta y_E &= (L_1\cos q_1 + L_2\cos(q_1+q_2))\delta q_1 \\ &\quad + L_2\cos(q_1+q_2)\delta q_2 \end{aligned} \tag{10}$$

The external force vector is defined as follows

$$\mathbf{Q}^* = \begin{bmatrix} -P_L(L_1\cos q_1 + L_2\cos(q_1+q_2)) \\ -P_L L_2\cos(q_1+q_2) \end{bmatrix} \tag{11}$$

Thus, the inverse dynamics equation is described as

$$\boldsymbol{\tau} = \mathbf{M}(\mathbf{q})\ddot{\mathbf{q}} + \mathbf{C}(\mathbf{q},\dot{\mathbf{q}})\dot{\mathbf{q}} + \mathbf{g}(\mathbf{q}) - \mathbf{Q}^* \tag{12}$$

The dynamic parameters of the 2DOF robot are described in Tab. 3.

TABLE III. DYNAMIC PARAMETERS OF THE 2DOF ROBOT

Parameters	Symbols (unit)	Value	
		Pre-TO	After-TO
Length of link 1	$L_1(m)$	0.25	
Length of link 2	$L_2(m)$	0.19	
Mass of link 1	$m_1(kg)$	1	
Mass of link 2	$m_2(kg)$	0.448	0.249
Mass of the object	$m_{Load}(kg)$	1	
Gravity center position vector of link 1	$\begin{bmatrix} L_{G1} & 0 & 0 \end{bmatrix}^T(m)$	$\begin{bmatrix} 0.115 & 0 & 0 \end{bmatrix}^T$	
Gravity center position vector of link 2	$\begin{bmatrix} L_{G2} & 0 & 0 \end{bmatrix}^T(m)$	$\begin{bmatrix} 0.097 & 0 & 0 \end{bmatrix}^T$	$\begin{bmatrix} 0.074 & 0 & 0 \end{bmatrix}^T$
Inertia moment of link 1 in OZ	$I_{1Z}(kgm^2)$	5.81×10^{-3}	
Inertia moment of link 2 in OZ	$I_{2Z}(kgm^2)$	1.94×10^{-3}	0.067×10^{-3}

Construct the motion trajectory of the robot through the trajectory of point E. It should be noted that the trajectory described below is the trajectory used for dynamic analysis in Section 2.1 and Section 2.2. The start position is

Duong Xuan Bien, Pham Dac Phong, Pham Hoang Nam, and Le Thanh Hung, "Inverse Dynamics Analysis of the Robot Arm Using the Topology Optimization," *International Research Journal of Advanced Engineering and Science*, Volume 8, Issue 1, pp. 267-272, 2023.

International Research Journal of Advanced Engineering and Science
ISSN (Online): 2455-9024

$\mathbf{x}_{0E} = \begin{bmatrix} 0.45 & 0 \end{bmatrix}^T$ corresponding to $\mathbf{q}_0 = \begin{bmatrix} 0 & 0 \end{bmatrix}^T$, the end position of the trajectory is $\mathbf{x}_{fE} = \begin{bmatrix} -0.1 & 0.27 \end{bmatrix}^T$ corresponding to $\mathbf{q}_f = \begin{bmatrix} \frac{5\pi}{6} & \frac{5\pi}{9} \end{bmatrix}^T$. The initial velocity of the joints is $\dot{\mathbf{q}}_0 = \begin{bmatrix} \frac{\pi}{12} & \frac{\pi}{18} \end{bmatrix}^T$. The motion time of the robot is $10(s)$. The trajectory of point E is depicted in Fig. 14. The position, velocity and acceleration of the joints are shown in Fig. 15, 16 and Fig. 17. The calculating results of the joints torque according to Eq. (12) are shown in Fig. 18 and Fig. 19.

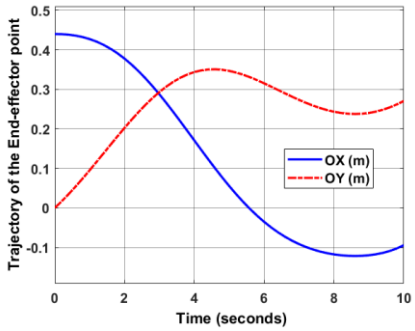

Fig. 14. Trajectory of the end-effector point

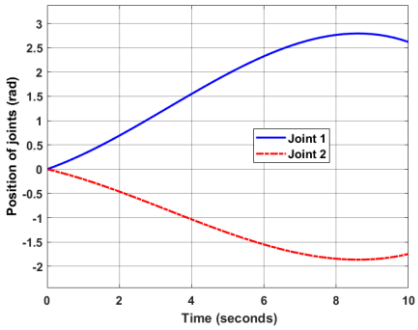

Fig. 15. Position of joints

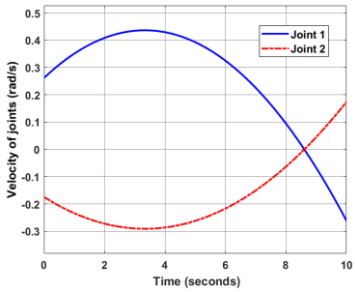

Fig. 16. Velocity of joints

The simulation results in Fig. 18 and Fig. 19 show that the torque value at the joints has a great change before and after the optimization of the link 2 structure. The torque value is significantly reduced in both joints. This shows that the energy requirements of the joints are reduced, and the working intensity of the joints also decreases. The maximum value of driving torque at the joints in the two cases before and after the optimum corresponding to the specific trajectory is shown in Tab. 4.

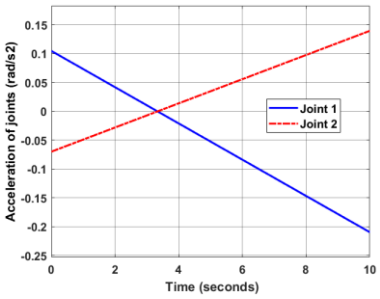

Fig. 17. Acceleration of joints

TABLE IV. COMPARISON OF MAXIMUM TORQUE VALUES

Cases	Torque value (Nm)	
	Joint 1	Joint 2
Pre-TO	1.68	0.43
After-TO	0.95	0.18
Deviation	Reduced 43.45%	Reduced 58.14%

Accordingly, the service life of joints tends to increase. Furthermore, the choice of the motor for the transmission of the joints can also be considered with the need for power not greater than in the case of without optimization of the structure.

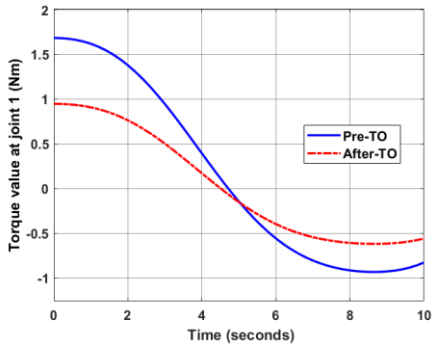

Fig. 18. Torque values at joint 1

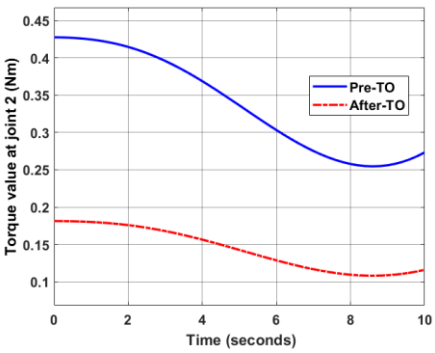

Fig. 19. Torque values at joint 2

III. CONCLUSIONS

The torque value at the joints of the two-link planar robot is specifically determined in this paper with two cases pre-TO

Duong Xuan Bien, Pham Dac Phong, Pham Hoang Nam, and Le Thanh Hung, "Inverse Dynamics Analysis of the Robot Arm Using the Topology Optimization," *International Research Journal of Advanced Engineering and Science*, Volume 8, Issue 1, pp. 267-272, 2023.

and after-TO applying the TO technique for the link 2. The maximum force and torque values at joints are calculated by static and dynamic analysis problem. Accordingly, the maximum stress and displacement values are also determined and serve as the basis for establishing optimal structural design criteria. Based on the results of static analysis and dynamic analysis of the 2DOF robot model, the SIMP algorithm is used to optimize the link 2 structure with a mass reduction of over 40% compared to the original mass. A motion trajectory is established in the joint space that corresponds to the motion trajectory in the workspace used in the pre-optimum dynamic analysis. The results of comparing force/moment values and stress/displacement values of the robot in dynamics analyzing show that the link 2 structure in the after-TO meets the criteria set out initially. The kinematics and dynamics equations of the robot are also established for two cases based on the mathematical model and the DH parameters. The results of the IK calculation show that the torque value based on the given robot's motion trajectory is significantly reduced by over 43% compared to the suboptimal time. This is important in selecting the most suitable drive motors and prolonging the life of the joints. Furthermore, the significant reduction in energy consumption driving at joints is an important factor in reducing the overall cost when applying robots for various tasks in manufacturing.

REFERENCES

[1] Y. Liu, X. Tian, "Robot path planning with two-axis positioner for non-ideal sphere-pipe joint welding based on laser scanning", *The International Journal of Advanced Manufacturing Technology*, 105 (1–4), 2019, pp. 1295–1310.

[2] L. Liang, J. Zhao, S. Ji, "An iterative feed rate scheduling method with confined high-order constraints in parametric interpolation", *The International Journal of Advanced Manufacturing Technology*, 92 (5–8), 2017, pp. 2001-2015.

[3] T. Sterling, H. Chen, "Robotic welding parameter optimization based on weld quality evaluation", 6th Annual IEEE International Conference on CYBER Technology in Automation, Control, and Intelligent Systems, 2016, pp. 216–221.

[4] R. R. Garcia, A. C. Bittencourt, E. Villani, "Relevant factors for the energy consumption of industrial robots", *Journal of the Brazilian Society of Mechanical Sciences and Engineering*, 40 (9), 2018, pp. 1–15.

[5] M. Paryanto, M. Brossog, Bornschlegl, J. Franke, "Reducing the energy consumption of industrial robots in manufacturing systems", *The International Journal of Advanced Manufacturing Technology*, 78 (5–8), 2015, pp. 1315-1328.

[6] C. A. My, D. X. Bien, C. H. Le, M. Packianather, "An efficient finite element formulation of dynamics for a flexible robot with different type of joints", *Mechanism and Machine Theory*, 134, 2019, pp. 267-288.

[7] M. Bendsoe, N. Kikuchi, "Generating Optimal Topologies in Structural Design Using a Homogenization Method", *Computer Methods in Applied Mechanics and Engineering*, 71, 1988, pp. 197-224.

[8] Y. M. Xie, G. P. Steven, "A Simple Evolutionary Procedure for Structural Optimization", *Computer & Structures*, 49 (5), 1993, pp. 885 - 896.

[9] M. P. Bendsoe, O. Sigmund, Topology Optimization - Theory, *Methods and Applications*, ISBN 3-540-42992-i Springer-Verlag Berlin Heidelberg New York, 2004.

[10] A. Erik, C. C. Anders, S. Mattias, S. L. Boyan, O. Sigmund, "Efficient topology optimization in MATLAB using 88 lines of code", *Structural and Multidisciplinary Optimization*, 43, 2011, pp. 1–16.

[11] H. L. Simonetti, V. S. Almeida, F. A. Neves, V. D. D. Almeida, "Topology Optimization for Elastic Analysis of 3D Structures using Evolutionary Methods", *Archives of Computational Methods in Engineering*, 2019, pp. 1-10.

[12] M. Y. Wang, X. Wang, D. Guo, "A level set method for structural topology optimization", *Computer Methods in Applied Mechanics and Engineering*, 192, 2003, pp. 227–246.

[13] S. Yan, Y. Bai, Y. Zhou, "Reduction of truss topology optimization", *Journal of Shanghai University* (English Edition), 13, 2009, pp. 489–496.

[14] P. Nilsson, Topology Optimization of a Swing Arm for a Track Driven Vehicle, Thesis at the Department of Physics, Umea University, Sweden, 2018.

[15] A. Albers, J. Ottnad, System Based Topology Optimization as Development Tools for Lightweight Components in Humanoid Robots, 8th IEEE-RAS International Conference on Humanoid Robots, Daejeon, Korea, 2008.

[16] N. Sagar, B. Esakki, Y. Lung-Jieh, U. Chandrasekhar, K. S. Vepa, "Design and Development of Unibody Quadcopter Structure Using Optimization and Additive Manufacturing Techniques", *Designs*, 6, 2022, pp. 1-25.

[17] B. Yunfei, C. Ming, L. Yongyao, "Structural Topology Optimization for a Robot Upper Arm Based on SIMP Method", *Mechanisms and Machine Science*, 36, 2016, pp. 725-733.

[18] X. Chu, H. Xu, G. Shao, W. Zheng, Multi-objective Topology Optimization for Industrial Robot, Proceedings of the IEEE International Conference on Information and Automation Ningbo, China, August, 2016.

[19] G. L. Srinivas, A. Javed, Multi-body dynamic optimization for upper arm of industrial manipulator, AIP Conference Proceedings 2281, 2020, 020022.

[20] M. Kumaran, V. Senthilkumar, Generative Design and Topology Optimization of Analysis and Repair Work of Industrial Robot Arm Manufactured Using Additive Manufacturing Technology, IOP Conference Series: Materials Science and Engineering, 1012, 2021, 012036.

[21] N. J. Reza, Theory Applied Robotics - Kinematics, Dynamics, and Control, Springer New York, ISBN 978-1-4419-1749-2, 2010.